Electron-lattice relaxation, and soliton structures and their interactions in polyenes.

Robert J. Bursill[1] and William Barford[2]
[1]*School of Physics, University of New South Wales, Sydney, NSW 2052, Australia.* [2]*Department of Physics and Astronomy, The University of Sheffield, Sheffield, S3 7RH, United Kingdom.*

Density matrix renormalisation group calculations of a suitably parametrised model of long polyenes (polyacetylene oligomers), which incorporates both long range Coulomb interactions and adiabatic lattice relaxation, are presented. The $1^3B_u^+$ and $2^1A_g^+$ states are found to have a 2-soliton and 4-soliton form, respectively, both with large relaxation energies. The $1^1B_u^-$ state forms an exciton-polaron and has a very small relaxation energy. The relaxed energy of the $2^1A_g^+$ state lies below that of the $1^1B_u^-$ state. The soliton/anti-soliton pairs are bound.

PACS numbers:71.10.F, 71.20.R, 71.35

Electronic interactions in polyenes and polyacetylene (PA) induce strong spin-density-wave correlations in the ground state, resulting in low energy spin-flip (or covalent) triplet ($^3B_u^+$) excitations. These combine to form even-parity (dipole-forbidden) singlet ($^1A_g^+$) excitations. Optical (dipole-allowed) transitions to the odd-parity singlet state ($^1B_u^-$) are essentially ionic in character, resulting in charge transfer from one site to another. In the non-interacting limit the $1^3B_u^+$ and $1^1B_u^-$ states are degenerate, and the $2^1A_g^+$ state always lies higher in energy. However, electron correlations can lead to a reversal of the energetic ordering of the $1^1B_u^-$ and $2^1A_g^+$ states. Electron-electron correlations in π conjugated systems, such as PA, are conveniently modelled by the one-band Pariser-Parr-Pople (P-P-P) model, which includes long range Coulomb interactions.

Electron-phonon interactions in the non-interacting limit are described by the SSH model. In the adiabatic limit it predicts a wealth of non-linear excitations, including charged/spinless ($S^{\pm}$) and neutral/spin 1/2 (S^{σ}) solitons. It is the inter-play of both electron-electron and electron-phonon interactions in PA which leads to an extremely rich variety of excitations. To describe these excitations we employ the density matrix renormalisation group (DMRG) [1] method to solve the P-P-P-SSH model, and utilise the Hellmann-Feynman (H-F) theorem to calculate the low-lying excited states and the lattice relaxation associated with them.

Earlier work on the solitonic structure of the low-lying excitations include, a renormalisation group calculation of the Hubbard-SSH model of up to 16 sites [2]; a mean-field study of the Heisenberg-Peierls model [3]; an exact diagonalisation of a 12 site extended Hubbard-SSH model [4]; and a strong coupling and perturbation calculation of the Hubbard-SSH model [5]. The DMRG method has recently been used by and Yaron et al. [6] and Fano et al. [7] to solve the P-P-P model for linear and cyclic polyenes, respectively. Jeckelmann [8] studied the metal-insulator transition in doped PA by solving the extended Hubbard-SSH with the DMRG method. Likewise, Kuwabara et al. [9] used the DMRG method to study the relative stability of bipolarons using the same model.

The P-P-P-SHH Hamiltonian is defined as

$$\begin{aligned}\mathcal{H} = &-2\sum_{i=1}^{N-1} t_i \hat{T}_i + \frac{1}{4\pi t_0 \lambda}\sum_{i=1}^{N-1}\Delta_i^2 + \Gamma\sum_{i=1}^{N-1}\Delta_i \\ &+ U\sum_{i=1}^{N}\left(n_{i\uparrow}-1/2\right)\left(n_{i\downarrow}-1/2\right) \\ &+ \frac{1}{2}\sum_{i\neq j}^{N} V_{ij}(n_i-1)(n_j-1), \end{aligned} \tag{1}$$

where, $t_i = \left(t_0 + \frac{\Delta_i}{2}\right)$ and $\hat{T}_i = \frac{1}{2}\sum_\sigma (c^\dagger_{i+1\sigma}c_{i\sigma} + h.c.)$ is the bond order operator of the ith. bond. We use the Ohno function for the Coulomb interaction: $V_{ij} = U/\sqrt{1+\beta r_{ij}^2}$, where $\beta = (U/14.397)^2$ and bond lengths are in Å. The single and double bond lengths used in the evaluation of V_{ij} are 1.46 Å and 1.35 Å, respectively, and the bond angle is 120^0. Various semi-empirical parametrisations exist for t_0 and U. We adopt the values which are optimal for benzene [10], whose C-C bond length of 1.40 Å is almost the same as the average bond length in PA thin films, i. e., $t_0 = 2.539$ eV and $U = 10.06$ eV. The dimensionless electron-phonon coupling constant, λ, is defined by $\lambda = 2\alpha^2/\pi K t_0$, where K is the elastic spring constant (estimated to be 46 eV $\mathring{A}^{-2}$ [11]), and α relates the actual distortion of the ith. bond from equilibrium, y_i, to Δ_i: $y_i = \Delta_i/2\alpha$. Γ is chosen so that the relaxed ground state of an infinite polymer has the same chain length as the unrelaxed state, i. e., $\sum_{i=1}^{N-1}\Delta_i = 0$. This ensures that the average hopping integral is t_0, which is applicable to C-C bond lengths of 1.40 Å. However, the chain length is permitted to change for excited states, and for all the states of finite oligomers. The remaining parameter, λ, is chosen so that the model fits the *vertical* excitation energies of the $1^1B_u^-$ and $2^1A_g^+$ states of hexatriene in the gas phase [12]. A choice of $\lambda = 0.115$ and $\Gamma = 0.602$ gives 4.965 eV and 5.212 eV,

compared to the experimental values of 4.96 eV and 5.21 eV, for the $1^1B_u^-$ and $2^1A_g^+$ states, respectively.

The equilibrium values of the bond length distortion are determined by the H-F condition that,

$$\frac{\partial E(\{\Delta_i\})}{\partial \Delta_i} = 0 \Rightarrow \Delta_i = 2\pi t_0 \lambda \left[\langle \hat{T}_i \rangle - \Gamma\right]. \qquad (2)$$

$\mathcal{H}$ possesses spatial reflection, particle-hole and spin-flip symmetries. Symmetrised eigenstates of $\mathcal{H}$ are constructed by an efficient process which makes use of the fact that the block symmetry operators commute with the density matrix at all stages of the calculation and which has been tested by making comparisons with exaxt results [13,14].

The calculation of the relaxed energy of a given state for a given chain length is as follows: (1) The eigenstate is calculated for an initial choice of $\{t_i\}$ by building up the lattice to the target chain size using the infinite lattice algorithm of the DMRG method. (2) At the target chain size the H-F condition (2) is repeatedly applied until the $\{t_i\}$ have converged. (3) Using the new values of $\{t_i\}$, steps 1 and 2 are repeated. The procedure is succesfully terminated when the energies have converged after successive lattice and H-F iterations. It is necessary to sweep through the lattice after each set of H-F iterations to ensure that the electronic states and the lattice geometry have converged simultaneously.

The accuracy of the DMRG implementation has been checked in a number of ways. First, the method has been compared with exact results in the non-interacting ($U = 0$) limit. The convergence of the ground state energy with superblock Hilbert space size (SBHSS) is shown in Table I for the $N = 102$ site system with various lattice geometries. The total energy converges to within 0.005 eV which is sufficient for energy gaps, which are of the order of 1 eV, to be resolved to within 1% or better. This represents the DMRG at its least accurate, as the addition of correlations improves convergence, as can be seen in Table II, where we present the DMRG convergence for the ground state energy and a number of energy gaps.

Using the ground state geometry, the vertical energies ($E^{\rm v}$) of the $1^3B_u^+$, $1^1B_u^-$ and $2^1A_g^+$ states are calculated. These, as well as the relaxed energies ($E^{\rm 0\text{-}0}$), are shown in Fig. 1 as functions of $1/N$. We first note that the vertical energies of the $1^1B_u^-$ and $2^1A_g^+$ states are very close, with a crossing at short chains, and again for long chains. In the thermodynamic limit $E^{\rm v}(1^1B_u^-) < E^{\rm v}(2^1A_g^+)$. This large N crossing has also been observed in the U-V dimerised Hubbard model [14,17].

The relaxation energy of the $1^1B_u^-$ state is modest (ca. 0.3 eV) and has not converged (i. e. it is still rapidly decreasing) for N = 102. By contrast, the relaxation energies of the $1^3B_u^+$ and $2^1A_g^+$ states are substantial, being ca. 0.5 eV and 1.0 eV, respectively, and converge rapidly with N. We have also calculated the energy of the $2^1A_g^+$ state using the relaxed geometry of the $1^1B_u^-$ state. This always lies lower than $E^{\rm 0\text{-}0}(1^1B_u^-)$, which implies that a vertical photo-excitation to the $1^1B_u^-$ state will decay to the $2^1A_g^+$ state. Finally, the experimental values of $E^{\rm 0\text{-}0}(1^1B_u^-)$ and $E^{\rm 0\text{-}0}(2^1A_g^+)$ for $N = 10$ and 14 are shown [15]. The $2^1A_g^+$ values are in good agreement with our calculation. The $1^1B_u^-$ values are ca. 0.3 eV lower than our predictions. The experimental results for $N =$ 8–14 have been analysed by Kohler [15]. For the $2^1A_g^+$ state the empirical relation $E^{\rm 0\text{-}0}(2^1A_g^+) = 0.96 + 20.72/N$ was derived, in good agreement with the photoinduced absorption result ca. 1.1 eV for polyacetylene thin films. However, Fig. 1 suggests that an algebraic fitting form is incorrect—the true scaling behaviour is exponential, and can only be seen by considering sufficiently large systems.

In Fig. 2 we plot as a function of bond index from the center of the chain, the normalised staggered bond dimerisation, defined as, $\delta_i \equiv (-1)^i(t_i - \bar{t})/\bar{t}$, where $\bar{t}$ is the average value of t_i in the middle of the chain [16]. Note that the $1^3B_u^+$ and $2^1A_g^+$ states undergo considerable bond distortion, whereas the $1^1B_u^-$ state and the charged state (denoted E_g) show a weak polaronic distortion of the lattice. The oscillatory behaviour of δ_i in the polaronic distortions indicates a local expansion of the lattice.

We fit the $1^3B_u^+$, $1^1B_u^-$ and charged state to a 2-soliton form [5,18],

$$\delta_i = \bar{\delta}\left\{1 + \tanh\left(2x_0/\xi\right)\left[\tanh\left((i - x_0)/\xi\right)\right.\right. \\ \left.\left. - \tanh\left((i + x_0)/\xi\right)\right]\right\}. \qquad (3)$$

The $2^1A_g^+$ state, however, evidently requires a 4-soliton [5,18] fit of the form,

$$\delta_i = \bar{\delta}\left\{1 + \tanh\left(2x_0/\xi\right)\left[\tanh\left((i - x_d - x_0)/\xi\right)\right.\right. \\ - \tanh\left((i - x_d + x_0)/\xi\right) + \tanh\left((i + x_d - x_0)/\xi\right) \\ \left.\left. - \tanh\left((i + x_d + x_0)/\xi\right)\right]\right\}. \qquad (4)$$

These functions give good fits to the relaxed geometries of the $N = 102$ site system, as shown in Fig. 2. The difference in energy between using the fits and the actual relaxed geometry is around 0.01 eV. The 4-soliton character of $2^1A_g^+$ state indicates the strong inter-play between electron-lattice relaxation and electron-electron correlations in polyenes, for, as indicated earlier, this state has a considerable triplet-triplet character.

Fig. 3 depicts the convergence of the various fitting parameters as a function of N. The $1^3B_u^+$ and $2^1A_g^+$ states converge rapidly with N, whereas the $1^1B_u^-$ state shows strong finite-size effects, and the coherence length ξ only begins to converge at around $N = 102$. The fact that the soliton structures converge with N leads to two important observations: First, the soliton/anti-soliton pair are bound, because if they were not their separation x_0 would increase with N. Second, the soliton structures are pinned in the middle of the lattice. This is a consequence of the classical adiabatic treatment of the lattice,

and is one of the reasons why the energy curves flatten off rapidly as $N \to \infty$.

To further investigate the soliton/anti-soliton interactions, adiabatic potential energy curves [5] (i. e. the energy as a function of soliton separation, x_0) are plotted in Fig. 4. Our results differ qualitatively from previous approximate calculations [5] in that the $1^1B_u^-$ and $1^3B_u^+$ are bound—the potentials have a minimum and are attractive for large x_0. This attractive soliton/anti-soliton interaction implies much stronger binding for the $2^1A_g^+$ state than that obtained in [5], where the binding energy was found to be ca. 0.05 eV. It should be noted, however, that [5] uses a Hamiltonian with short ranged (on-site) interactions, with the strength chosen so as to fit the vertical absorption peak in polyacetylene thin films. Furthermore, our calculations, being for polyenes, necessarily use open boundary conditions. For an even site chain there is one more short bond than there are long bonds. This means that the ground state is non-degenerate, as it is energetically unfavourable to swap long and short bonds, and is one reason for the long range confinement. The rôle played by boundary conditions is subtle and important, as real systems, such as oligomers and polymers with disorder, have a finite conjugation length.

Another consideration is the adequacy of the soliton fits used in generating the adiabatic energy curves. We consider the generalised potential energy curves where, for a given x_0, we allow ξ to vary so as to minimise the energy. Results for the $1^1B_u^-$ state are included in Fig. 4, which show that relaxing ξ yields a substantial reduction in the energy, implying weak soliton/anti-soliton binding. However, the energy reduction for the $1^3B_u^+$ state is insignificant over the range of x_0 values plotted, indicating that there is a stronger binding of the solitons in the $2^1A_g^+$ and $1^3B_u^+$ states. A further generalisation of the soliton fits would be to consider multiple soliton/anti-soliton pairs.

Finally, we note the consequences of our results for the interpretation of experiments. Our results for small polyenes are in good agreement with experiment—the energy difference of ca. 0.3 eV for the $1^1B_u^-$ state can probably be explained by solvation effects [19], supporting the notion that the covalent $2^1A_g^+$ state is less polarised than the ionic $1^1B_u^-$. In the bulk limit the $1^1B_u^-$ and $2^1A_g^+$ energies are ca. 0.8 eV higher than data from linear [20] and 2-photon [21] absorption and third harmonic generation [22] experiments on PA thin films. This implies that there are more substantial energy decreases due to solvation and aggregation (interchain hopping and eximer formation) effects. Such effects must be investigated via coupled chain calculations. Also, the neglect of quantum fluctuations in the adiabatic treatment of the lattice [23], leading to the pinning of the soliton structures, will contribute to this energy difference. A full treatment must include dynamical phonons. Such a treatment would also increase our understanding of the soliton confinement.

R. J. B. was supported by the Australian Research Council. W. B. gratefully acknowledges financial support from the Royal Society and the Gordon Godfrey Bequest of the UNSW. We thank E. Jeckelmann and Y. Shimoi for useful discussions. The calculations were performed at the New South Wales Center for Parallel Computing.

---

* Email address: ph1rb@newt.phys.unsw.edu.au; w.barford@sheffield.ac.uk

[1] S. R. White, Phys. Rev. Lett. **69**, 2863 (1992); Phys. Rev. B **48**, 10345 (1993).
[2] G. W. Hayden and E. J. Mele, Phys. Rev. B **34**, 5484 (1986).
[3] J. Takimoto and M. Sasai, Phys. Rev. B **39**, 8511 (1989).
[4] J. T. Gammel and D. K. Campbell, Synth. Met. **55**, 4638 (1993).
[5] W. P. Su, Phys. Rev. Lett. **74**, 1167 (1995).
[6] D. Yaron, E. E. Moore, Z. Shuai, J. J. Bredas, J. Chem. Phys. **108**, 7451 (1998).
[7] G. Fano, F. Ortolani, L. Ziosi, J. Chem. Phys. **108**, 9246 (1998).
[8] J. Jeckelmann, Phys. Rev. B **57**, 11 838 (1998).
[9] M. Kuwabara, Y. Shimoi, S. Abe, J. Phys. Soc. Jpn. **67**, 1521 (1998).
[10] R. J. Bursill, C. Castleton, W. Barford, Chem. Phys. Lett. **294**, 305 (1998).
[11] E. Ehrenfreund, Z. Vardeny, O. Barfman, B. Horovitz, Phys. Rev. B **36**, 1535 (1987).
[12] W. M. Flicker, O. A. Mosher and A. Kuppermann, Chem. Phys. Lett. **45**, 492 (1977).
[13] M. Boman, R. J. Bursill and W. Barford, Synth. Met. **85**, 1059 (1997).
[14] M. Boman and R. J. Bursill, Phys. Rev. B **57**, 15 167 (1998).
[15] B. E. Kohler, J. Chem. Phys. **88**, 2788 (1988).
[16] We have checked the DMRG convergence of the δ_i and found that, for the $N = 102$ site lattice, they are resolved to within 1% or less.
[17] Z. Shuai, J. L. Bredas, S. K. Pati and S. Ramasesha, Phys. Rev. B **56**, 9298 (1997).
[18] D. K. Campbell and A. R. Bishop, Nucl. Phys. B **200**, 297 (1982).
[19] E. Moore, B. Gherman B. and D. Yaron, J. Chem. Phys. **106**, 4216 (1997).
[20] Relaxation in Polymers (p 174), ed. by T. Kobayashi. World Scientific (Singapore) 1993.
[21] C. Halvorson and A. J. Heeger, Chem. Phys. Lett. **216**, 488 (1993).
[22] W. S. Fann, *et al.*, Phys. Rev. Lett. **62**, 1492 (1989).
[23] R. H. McKenzie and J. W. Wilkins, Phys. Rev. Lett. **69** 1085 (1992).

TABLE I. Convergence of the ground state energy (in eV) as a function of the SBHSS for the $N = 102$ site system in the non-interacting case ($U = 0$) for three geometries defined by the soliton form (3), taking $\xi = 4.03$ and (i) $x_0 = 0$ (uniformly dimerised geometry), (ii) $x_0 = \infty$ (uniformly dimerised with long and short bonds reversed), and (iii) $x_0 = 24.87$ (a geometry with a kink/anti-kink pair placed 1/4 and 3/4 of the way along the lattice). m is the number of states retained per block.

m	SBHSS	$x_0 = 0$	$x_0 = \infty$	$x_0 = 24.87$
75	5920	−332.57146	−330.205	−331.333
100	9384	−332.57217	−330.403	−331.366
150	22392	−332.57257	−330.426	−331.407
200	37512	−332.57271	−330.439	−331.422
230	52312	−332.57272	−330.446	−331.428
270	72392	−332.57273	−330.448	−331.430
EXACT	—	−332.57276	−330.452	−331.434

TABLE II. Convergence of the ground state ($1^1A_g^+$) energy and vertical and 0-0 transition energies of the $2^1A_g^+$ and $1^1B_u^-$ states as a function of the SBHSS for the $N = 102$ site system.

SBHSS	$1^1A_g^+$	$2^1A_g^+$	$2^1A_g^+$(0-0)	$1^1B_u^-$	$1^1B_u^-$(0-0)
15844	−509.6330807	2.8927	1.8051	2.7719	2.6785
25492	−509.6330971	2.8795	1.8008	2.7650	2.6483
36312	−509.6331002	2.8764	1.7972	2.7617	2.6392
54916	−509.6331009	2.8744	1.7963	2.7605	2.6345
67240	−509.6331010	2.8737	1.7959	2.7601	2.6336

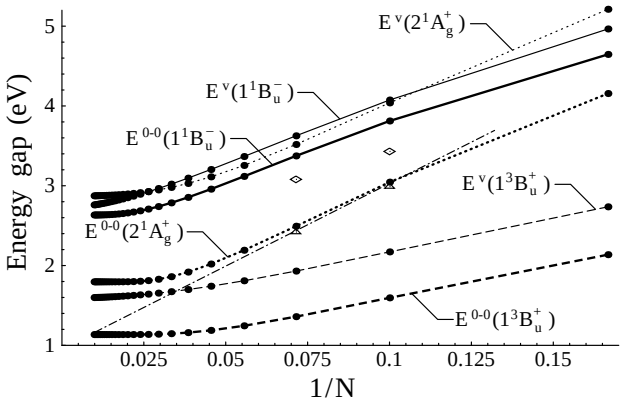

FIG. 1. Energy gaps for the $1^1B_u^+$ (solid lines) $2^1A_g^+$ (dotted lines) and $1^3B_u^+$ (dashed lines) states as a function of $1/N$. Vertical/0-0 transitions are indicated by thin/thick lines. Experimental 0-0 energies of the $1^1B_u^-$ (diamonds) and $2^1A_g^+$ (triangles) states for polyenes in hydrocarbon solution [15]. The empirical fitting form $E^{0\text{-}0}(2^1A_g^+) = 0.96 + 20.72/N$, derived in [15] from the 8–14-site oligomer data is also plotted (dot-dashed line).

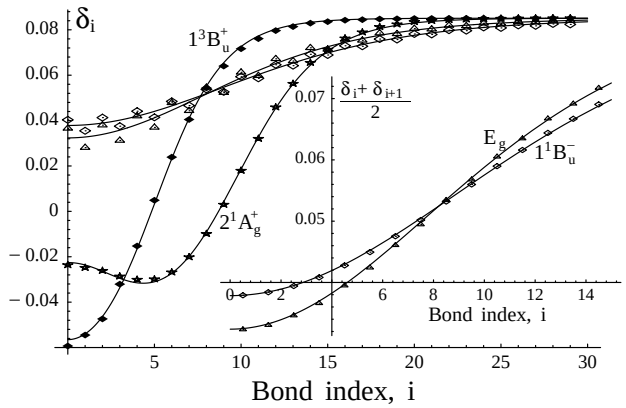

FIG. 2. The geometries (δ_i as a function of bond index i from the center of the lattice) of various excitations: $1^1B_u^-$ (open diamonds), $1^3B_u^+$ (filled diamonds), $2^1A_g^+$ (stars) and the charged state, E_g, (open triangles), for the $N = 102$ site system. The solid lines are fits to the 2-soliton form (3) (and the 4-soliton form (4) for the $2^1A_g^+$). The inset shows the two-point averages $((2i+1)/2, (\delta_i + \delta_{i+1})/2)$ for the polaronic E_g and $1^1B_u^-$ states, which are well described by the 2-soliton fits.

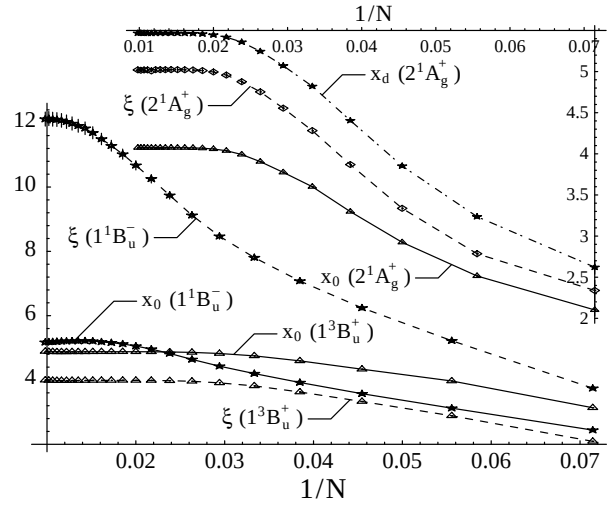

FIG. 3. The convergence of the soliton fitting parameters x_0 and ξ for the $1^1B_u^-$ and $1^3B_u^+$ states with the lattice size, N. The inset shows x_0, ξ and x_d for the $2^1A_g^+$ state.

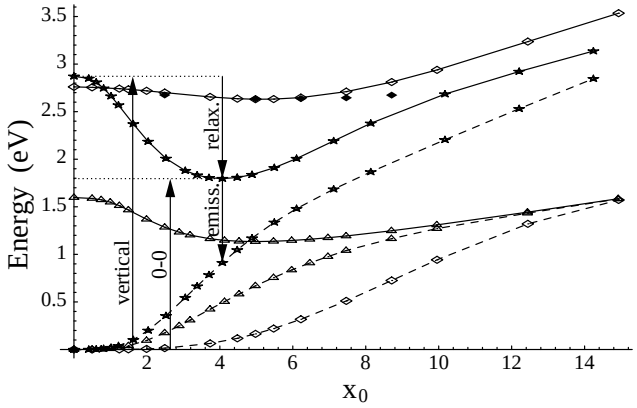

FIG. 4. Potential energy curves (solid lines) for the $1^1B_u^-$ (diamonds), $2^1A_g^+$ (stars) and $1^3B_u^+$ (triangles) states for the $N = 102$ site lattice. The dashed curves are the corresponding ground state ($1^1A_g^+$) potential energies. For the $1^1B_u^-$ and $1^3B_u^+$ cases, the curves are generated using the soliton pair form (3) with the fitted values of ξ (4.01 and 12.12, respectively) and varying x_0. For the $2^1A_g^+$ case the curves are generated using the 4-soliton form (4) with the fitted value $\xi = 4.93$ and varying x_0. x_d is chosen so that the ratio x_d/x_0 remains fixed at its fitted value of 1.35. The solid diamonds are the values of the $1^1B_u^-$ energy when ξ is also allowed to vary. The energies of the vertical, 0-0 and emission transitions, and the relaxation energy can be read off from this plot. This is illustrated using arrowed vertical lines for the $2^1A_g^+$ state.